# Structural Properties of Fibril-forming Segments of α-Synuclein

**Jeseong Yoon, Joonho Park, Soonmin Jang,† Kyunghee Lee,† and Seokmin Shin***

*School of Chemistry, Seoul National University, Seoul 151-747, Korea. *E-mail: sshin@snu.ac.kr*
*†Department of Chemistry, Sejong University, Seoul 143-747, Korea*
*Received December 31, 2008, Accepted January 28, 2009*

We have performed replica-exchange molecular dynamics simulations on 41 residue peptide mainly composed of NAC (non Aβ component) sequence in α-Synuclein. To investigate conformational characteristics of intrinsically unstructured peptides, we carried out structural analysis on the 'representative structures' for ensemble of structures occurring at different temperatures. The secondary structure profile obtained from our simulations suggests that the NAC region of α-synuclein can be divided into roughly three helical-like segments. It is found that the overall helix-turn-helix like topology is conserved even though the conformational fluctuations grow as the temperature increases. The coordinate-based and the distance-based representative structures exhibit noticeable differences at higher temperatures while they are similar at lower temperatures. It is found that structural variations for the coordinate-based representative structures are much larger, suggesting that distance-based representative structures provide more reliable information concerning characteristic features of intrinsically unstructured proteins. The present analysis also indicates that the conformational features of representative structures at high temperatures might be related to those in membrane or low pH environment.

**Key Words**: Replica-exchange molecular dynamics, Fibril formation, α-Synuclein, Natively unstructured protein, Representative structure

## Introduction

Many neurodegenerative diseases such as Alzheimer's, Creutzfeldt-Jacob, and Parkinson's disease are known to be related with the formation of amyloid-like fibrils at neuronal surface.[1,2] Extensive experimental researches have been performed to reveal the pathologies of these diseases, in particular, the mechanism of formation of oligomers or fibrils.[3,4] Despite considerable advances in experimental works, detailed information concerning atomic level features of structures and formation mechanism of protein aggregates are rather limited. Part of the reason is due to the non-crystalline and insoluble nature of amyloid fibrils. More importantly, corresponding proteins are intrinsically unstructured and exhibit high conformational plasticity, which is very sensitive to environmental conditions.[5] The characteristics of the so-called "intrinsically unstructured" or "intrinsically disordered" proteins have been actively investigated in recent years.[6-8] There has been an increasing recognition that study of unfolded or partially folded states of natively or intrinsically unstructured proteins are essential to understanding some biological processes. Actually, numerous proteins lacking intrinsic globular structure under physiological condition have been recognized and many of them are found to be involved in important regulatory functions inside cell.[9] It is known that such inherent flexibility of those proteins acts as a functional advantage such that they can bind multiple targets depending on cell conditions. Rapid turnover in solution state allows the sensitivity of cell cycle to external conditions.[10] With a rapid increase in available computational resources, one of the most direct and prominent theoretical approaches to investigate the structural and dynamical aspects of protein misfolding aggregation on molecular level is to perform systematic molecular dynamics simulations.[11] Computational studies provide an integral part of multidisciplinary approaches for elucidating various amyloid assemblies.[12]

A number of recent observations implicate α-synuclein in the pathogenesis of Parkin's disease (PD).[13] In particular, the fibrillization of α-synuclein is the primary component of Lewy bodies (LBs) and Lewy neuritis (LNs) that are diagnostic hallmarks of PD.[14-16] It has been suggested that α-synuclein plays an important role in the pathogenesis of several neurodegenerative disorders. Experimental studies, based on circular dichroism (CD) or other optical methods, showed that α-synuclein did not appear to possess a well-defined native structure, making it a member of intrinsically unstructured proteins.[17,18] It was also noticed that α-synuclein exhibited a remarkable conformational plasticity depending on the environment.[19] The flexible structure of α-synuclein makes it versatile for its interaction with other proteins.[20] α-Synuclein was shown to adopt mostly helical secondary structure upon association with small unilamellar vesicles or detergent micelle surfaces.[17] The detailed structure and dynamics of micelle-bound α-synuclein were determined by NMR studies recently.[21] α-Synuclein is 140 residue protein primarily found in neural tissue, especially in presynaptic terminals. It is reported that the region called non-amyloid component (NAC) corresponding to 61-95 amino acid sequence of human α-synuclein plays a crucial role in fibril formation.[22]

In this work, we investigated conformational characteristics of a peptide mainly composed of NAC sequence of α-synuclein, which is known to be intrinsically unstructured and strongly hydrophobic. We performed replica-exchange molecular dynamics (REMD) on NAC peptide to sample the conformations more efficiently. In the previous work, we carried out structural analysis by introducing 'representative

structure' for ensemble of structures occurring during the overall trajectory.[23] It was found that representative structures can provide useful information about structural characteristics of intrinsically unstructured proteins such as α-synuclein. In the present work, the effect of temperature on stability and conformational change is examined in detail. The present study is expected to provide possible structural features of α-Synuclein with relation to fibril formation.

## Model and Simulation Details

We have performed replica-exchange molecular dynamics simulation on the residues 58-98 of human α-synuclein. N-terminal and C-terminal are blocked with Ace and Nme group, respectively. All-atom AMBER(parm98)[24] force field was used with with GB/SA implicit water model.[25] The solution pH is set to be neutral by default. Berendsen thermostat[26] for temperature control with coupling parameter 0.2ps and cutoff 9.0 Å was used during the whole simulation. Simulation was performed using TINKER package.[27] In our simulation, fully extended peptide of 41 residues was minimized and equilibrated for a several hundred picoseconds and after equilibration is achieved, conformations are randomly chosen from the trajectory to be used as initial conformations of each replica for REMD simulations. The number of replicas is 18 and the total length of simulation is 12 ns. The temperature distribution is 270, 284, 299, 314, 330, 348, 366, 385, 405, 426, 448, 471, 495, 521, 548, 577, 607, 638 (K). Among these, we used the trajectories corresponding to the first 9 temperatures for analysis. The exchange ratio between each neighboring pair of replicas are nearly uniform with the magnitudes in the range of 0.10 ~ 0.25. The time step is 2 fs and the coordinate is collected every 0.3 ps.

Secondary structure contents are obtained using DSSP program[28] and radius of gyration is calculated in TINKER package. Phi and Psi angles used to draw Ramachandran plot are also obtained from the result of DSSP program. The angles of terminal residues and glycine residues are neglected. The angle space between the maximum and minimum values are divided by 200 grids for Phi and Psi angles, respectively and the number of data is counted for each of 200 × 200 bins. For clear presentation of the Ramachandran plot, we plot $-RT\log N_{ij}$ instead of $N_{ij}$ where R is the gas constant, T is the temperature (K), and $N_{ij}$ is number of data in $(i,j)$-bin. For contact maps, we measured the distances between alpha carbon atoms for all pairs of residues. The distances are classified into 3 cases : $r \leq 6$ Å, 6 Å $< r \leq 8$ Å, and $r > 8$ Å, which are marked as different colors in contact map.

The time evolution of sampled PC (principle component) space can be a measure of the convergence of trajectory. To examine the convergence of trajectory for 299 K, we calculated the first two major principle components about alpha carbon coordinates of the whole trajectory and projected the trajectory onto the two principle axes. We divide the PC space into 50 × 50 grids, trace the projected trajectory in the PC space, and count the number of visited grids as a function of time. We used Ptraj module in AMBER9 to perform PC analysis.

In order to examine the conformational characteristics of a 'representative structure' for ensemble of structures occurring during the overall trajectory, we determined an average structure in two different ways.: first, we simply averaged the $C_\alpha$ coordinates of individual structures in the ensemble of structures, and calculated $C_\alpha$ RMSD value of each structure in the trajectory with respect to the coordinate averaged structure. The structure corresponding to the lowest RMSD value may be considered as the coordinate averaged representative structure. Least-square fitting of the structures is performed before averaging coordinates, using the McLachlan algorithm[29] which is implemented in the program ProFit.[30] RMSD calculation was carried out using MMTSB toolset.

The second way of analyzing ensemble of structures is to use distance matrix.[31] We calculated an inter-distance matrix for every possible $C_\alpha$ pairs for individual structure and obtained averaged distance matrix for the ensemble of structures. In order to compare the distance matrix of individual structure with the averaged distance matrix, we calculate the distance root-mean square deviation (dRMS) as

$$dRMS = \sqrt{2\sum_{i>j}\left[D_{ij}(x) - \bar{D}_{ij}\right]^2 \Big/ n(n-1)}$$

where $D_{ij}(x)$ refers to the distance between atoms $i$ and $j$ in structure $x$ and $\bar{D}_{ij}$ is the $ij$ component of the averaged distance matrix. The structure corresponding to the lowest dRMS value may be considered as the distance averaged representative structure.

## Results and Discussion

Fig. 1 and Table 1 show the temperature dependence of various secondary structural contents. Secondary structures usually show strong force field dependence. In particular, recent study showed that several versions of AMBER force fields produce different structural and thermodynamics properties and lead to force-field dependent folding mechanisms.[32] It should be noted that some of the results from the present calculations have intrinsic limitations attributed to the force

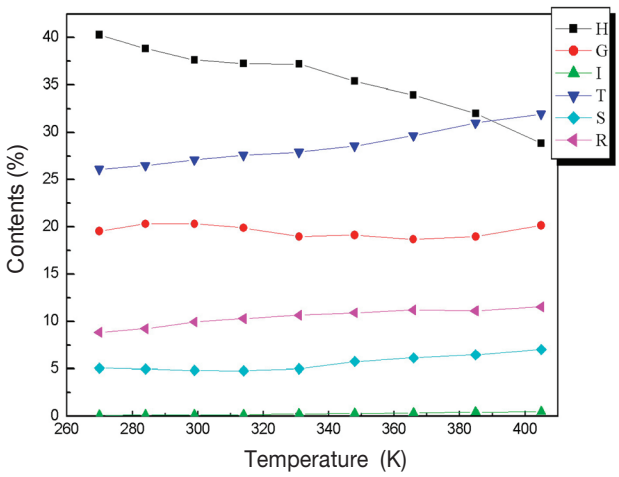


**Figure 1.** Temperature dependence of the fraction of secondary structure contents for NAC peptide of α-synuclein. H: α-helix, G: $3_{10}$-helix, I: π-helix, T: turn, S: bend, R: random coil.

field and solvation model used in the study. For example, high content of $3_{10}$-helix may be a force field artifact.[33,34] Even though the structures of α-synuclein are known to be mostly disordered without definite secondary structures, the secondary structure profile obtained from our calculations suggest that the NAC region can be divided into roughly three helical-like segments. This result is qualitatively consistent with experiment[35] and computational prediction of nonnative sequence propensity.[36] It is found that the α-helix content slightly decreases as the temperature is raised while the turn increases. On the contrary, it is also noted that the overall change of (α-helix + $3_{10}$-helix) content as a function of residue number is not so large when the temperature is varied. It can be concluded that the overall helix-turn-helix like topology is conserved even though the conformational fluctuations grow as the temperature increases.

Conservation of characteristic conformational features under temperature variation is also illustrated in the representative structures shown in Figs. 2 and 3. Fig. 2 shows distance-based representative structures at various temperatures. It is shown that conformational flexibility increases and the overall compactness decreases at higher temperatures, which is demonstrated by the increases in the average radius of gyrations as shown in Fig. 4. Fig. 5 shows the average solvent accessible surface area (SASA), which can provide additional information about the overall compactness and flexibility of the representative structures. The representative structures clearly suggest that the overall topological features - helices and turns - are not varied much as the temperature is raised. Fig. 3 shows coordinate-based representative structures at various temperatures. It is shown that the coordinate-based and the distance-based representative structures exhibit noticeable differences at higher temperatures while they are similar at lower temperatures. It can be argued that coordinate-based representative structures are poor in describing the overall topological features because it is difficult to obtain consistent

**Table 1.** The fraction of secondary structure contents (in %) for NAC peptide of α-synuclein, obtained from simulation trajectories at different temperatures.

| Temperature (K) | α-Helix | $3_{10}$-Helix | π-Helix | Turn | Bend |
|---|---|---|---|---|---|
| 270 | 40.3 | 19.55 | 0.11 | 26.1 | 5.09 |
| 284 | 38.84 | 20.33 | 0.14 | 26.5 | 4.97 |
| 299 | 37.63 | 20.33 | 0.14 | 27.12 | 4.84 |
| 314 | 37.25 | 19.89 | 0.16 | 27.6 | 4.79 |
| 331 | 37.2 | 18.98 | 0.25 | 27.92 | 5.0 |
| 348 | 35.39 | 19.13 | 0.28 | 28.56 | 5.75 |
| 366 | 33.96 | 18.68 | 0.35 | 29.66 | 6.15 |
| 385 | 32.0 | 18.97 | 0.42 | 31.01 | 6.48 |
| 405 | 28.87 | 20.15 | 0.47 | 31.95 | 7.03 |

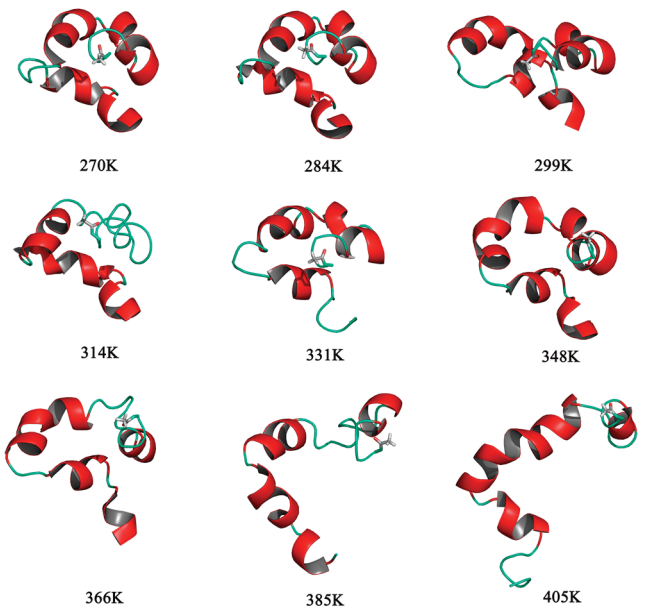


**Figure 2.** Distance averaged representative structures for NAC peptide of α-synuclein, obtained from simulation trajectories at different temperatures.

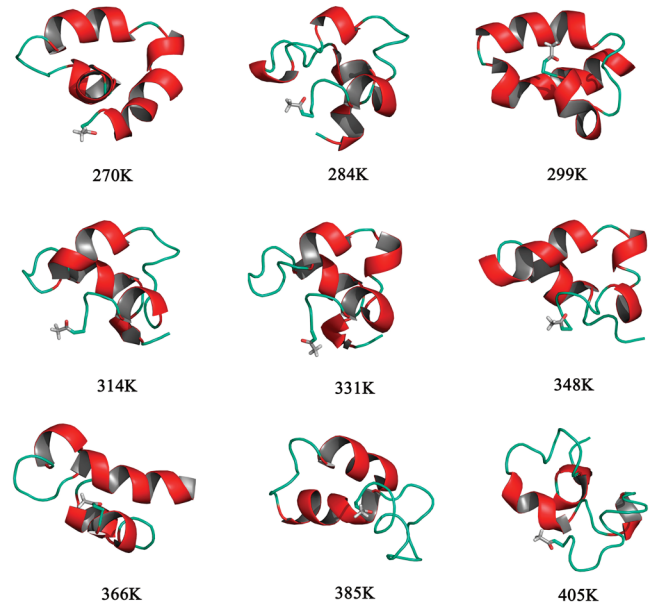


**Figure 3.** Coordinate averaged representative structures for NAC peptide of α-synuclein, obtained from simulation trajectories at different temperatures.

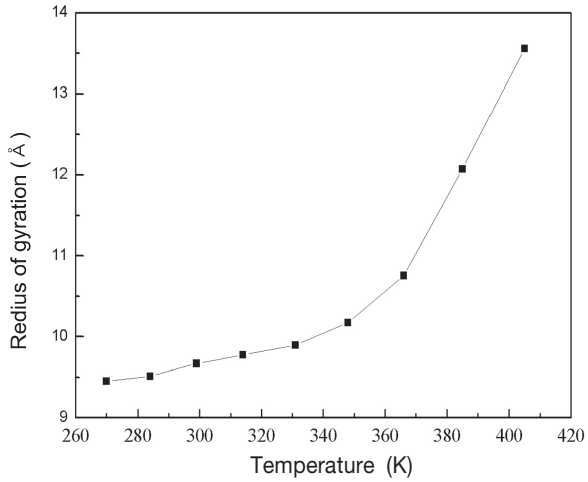


**Figure 4.** Temperature dependence of the average radius of gyration for NAC peptide of α-synuclein.

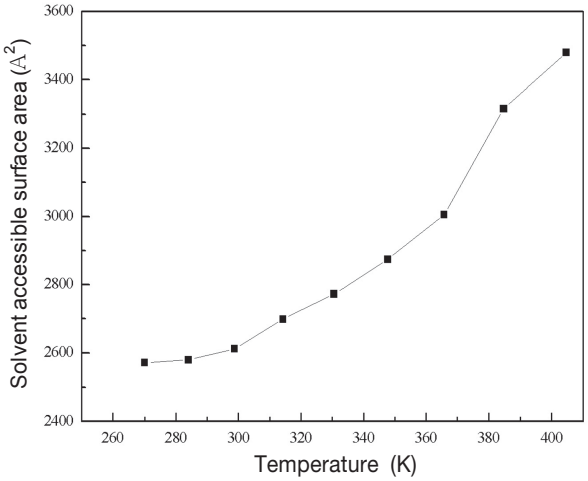


**Figure 5.** Temperature dependence of the average solvent accessible surface area (SASA) for NAC peptide of α-synuclein.

coordinate averaging due to large conformational fluctuations at higher temperatures. Table 2 shows the distances ($C_\alpha$-RMSD and dRMS) for the representative structures at different temperatures, compared with the representative structure of 299K, for distance-based and coordinate-based structures. It is found that structural variations for the coordinate-based representative structures are much larger. It can be concluded that distance-based representative structures provide more reliable information concerning characteristic features of intrinsically unstructured proteins.

**Table 2**. $C_\alpha$-RMSD and dRMS values for the representative structure of each temperature compared with the representative structure of 299 K.

| Temperature (K) | $C_\alpha$-RMSD | dRMS |
|---|---|---|
| 270 | 6.94 | 3.17 |
| 284 | 6.26 | 3.29 |
| 314 | 5.53 | 2.97 |
| 331 | 5.92 | 3.02 |
| 348 | 5.21 | 3.23 |
| 366 | 7.68 | 2.80 |
| 385 | 7.46 | 6.27 |
| 405 | 9.06 | 8.36 |

Figs. 6 and 7 show $C_\alpha$-distance contact map at each temperature with respect to distance-based and coordinate-based representative structures, respectively. It is found that as temperature is raised, the off-diagonal blocks, in particular, the broad cross-diagonal band regions at low temperatures

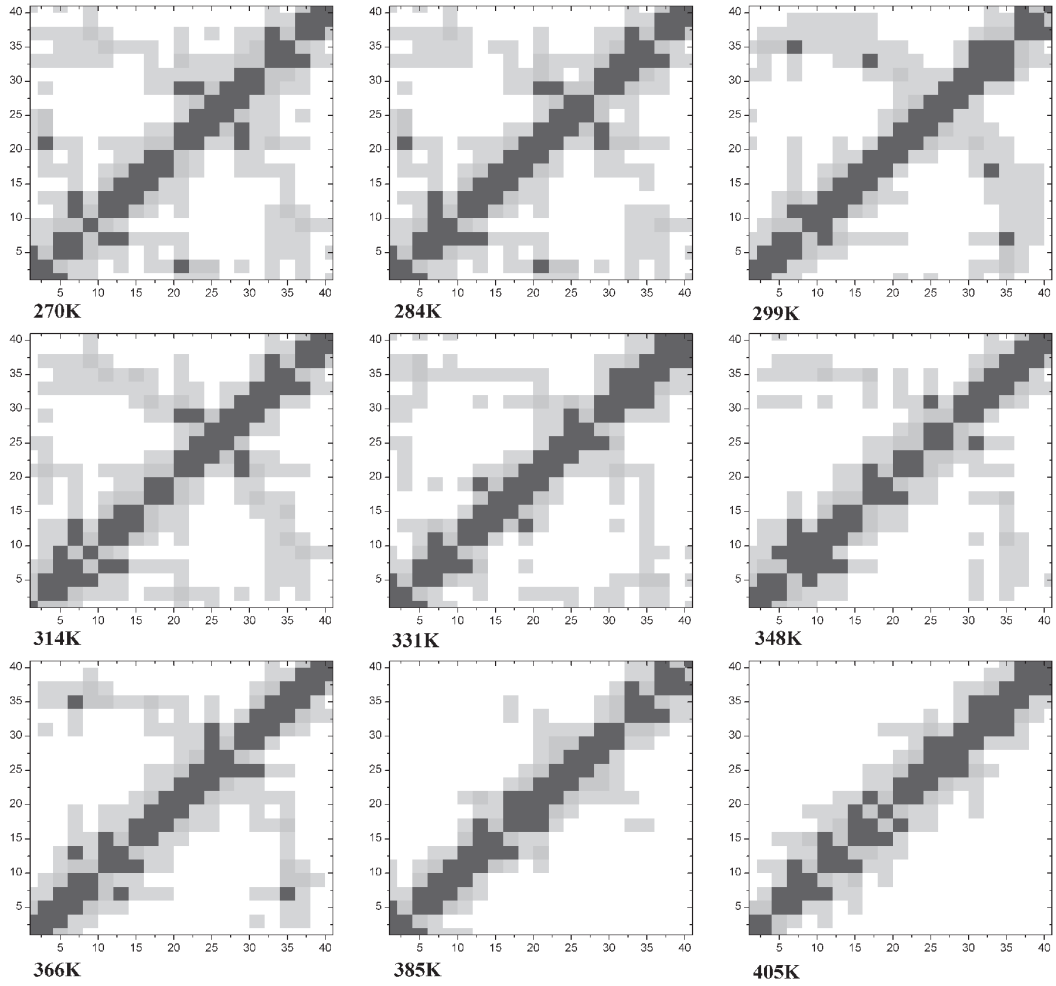


**Figure 6.** $C_\alpha$-$C_\alpha$ contact maps for distance-based representative structures of NAC peptide of α-synuclein, obtained from simulation trajectories at different temperatures.

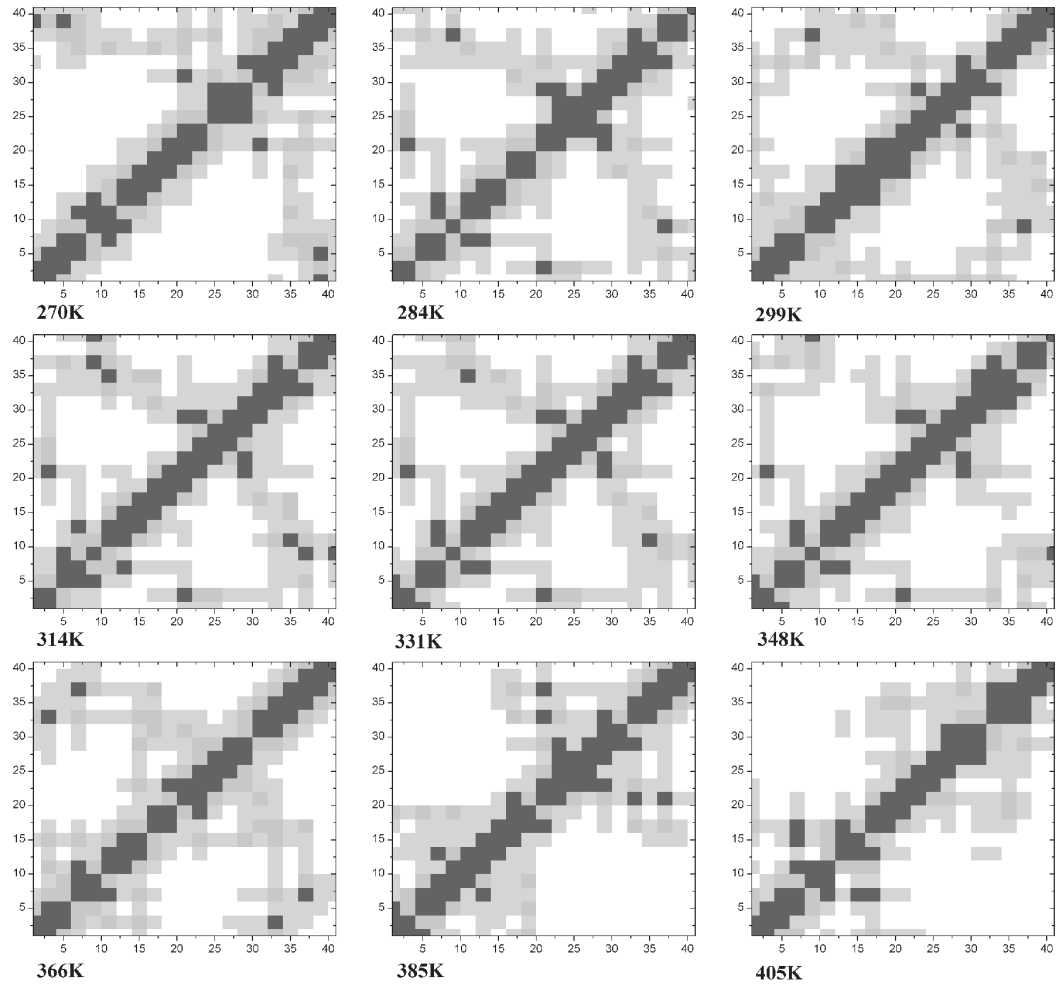


**Figure 7.** $C_\alpha$-$C_\alpha$ contact maps for coordinate-based representative structures of NAC peptide of α-synuclein, obtained from simulation trajectories at different temperatures.

disappear. It demonstrates that compact structures at low temperatures become expanded by heating along with the removal of 3-dimensional contacts between N-terminal and C-terminal regions. It should be noted that the overall conformational ensemble is highly unstructured: the average $C_\alpha$-RMSD value with respect to the coordinated-average structure is about 5-6 Å with large fluctuations.[23] This is consistent with the intrinsically unstructured properties of conformational ensemble, which is mainly contributed to the relatively weak contacts between different segments of the peptide. The representative structures described in the above illustrate that conformational characteristics such as local secondary structures and global topological features can be defined even for proteins with large conformational fluctuations.

Extended beta sheet and beta-bridge structures with characteristic hydrogen bonds may not be easily formed for the NAC peptide chain of 41 residues with highly hydrophobic sequence. Recently, El-Agnaf *et al.* showed through their biochemical analysis of the NAC peptide that NAC N-terminal region corresponding to amino acid residues 1-18 aggregates to form amyloid fibrils, while the C-terminal region with residues of 19-35 remains soluble and flexible.[37] It is suggested that the N-terminal region is responsible for the fibril formation. It is also known that the N-terminal region of α-synuclein consisting of 7 repeated units of 11 residues is predicted to form amphiphilic helices, while the C-terminal region enriched in acidic residues and prolines is expected to remain disordered.[38] It can be argued that the monomeric state of the NAC peptide does not exhibit beta-like structures with random conformations of C-terminal region and potentially helical conformations of N-terminal region.

Uversky *et al*. showed that a decrease in pH or an increase in temperature transform α-synuclein into a partially folded conformation.[39] It is suggested that this partially folded intermediate is critical for fibrillation. However, they did not identify the partially folded region exactly. Extensive experimental data support the hypothesis that pathological aggregation may arise from such partially folded intermediates. They are usually supposed to have sizable hydrophobic side chains on their surface, leading to aggregation facilitated by strong hydrophobic interactions.[38] Our results indicated that the NAC region seems to have a partially folded structure whose temperature dependence is rather weak. It is more likely that the region of α-synuclein, whose folding increases with temperature, is outside the NAC sequence. The increase in fibrillation rate at low pH may be attributed to the decrease in

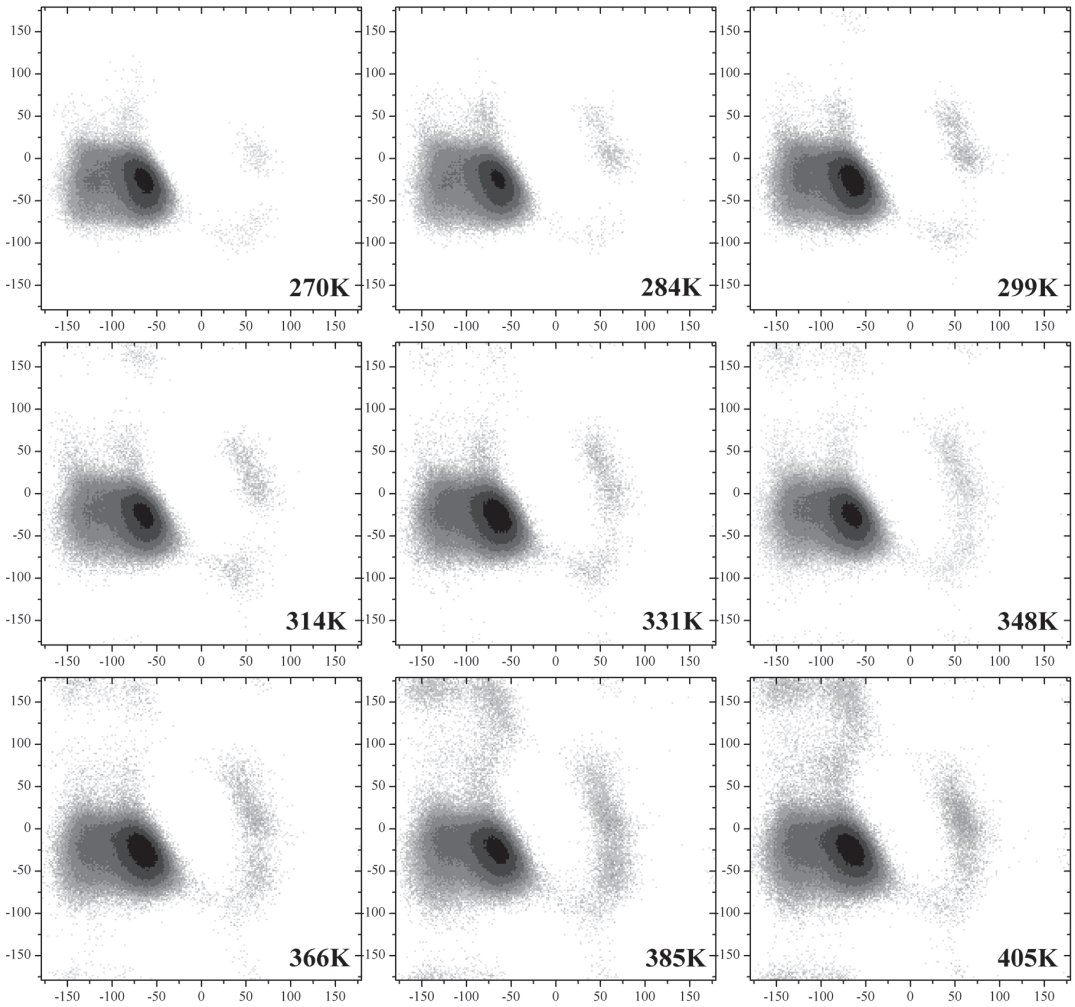


**Figure 8.** Ramachandran plots for NAC peptide of α-synuclein, obtained from simulation trajectories at different temperatures.

net charge, strengthening the intrinsic hydrophobicity and leading to partial folding. Elevated temperatures are also supposed to make similar effects. Recent experiment showed that a peptide composed of residues α-synuclein 71-82 itself can self assemble to form a fibril-like structure.[40] With respect to membrane association, it was reported that membranes accelerate the fibrillation.[41] It was also suggested that acidic lipid membranes may play the same role as low pH, leading to partial folding via decrease in net charge of N-terminal region of α-synuclein. It can be argued that the conformational features of representative structures at high temperatures might be related to those in membrane or low pH environment. Recently, Bisaglia *et al*. studied the structure and topology of NAC peptide in the membrane-mimetic environment.[42] It is found that in the membrane-mimetic environment, NAC peptide forms characteristic three regions of helical conformation with C-terminal region less stable. The lowest energy structures were calculated from NOE-based distance restraints and the backbone dihedral angles were derived from chemical shifts. It is noted that the resulting topological and geometrical features of the lowest energy structures are in close agreement with the representative structures at high temperatures in the present study. Fig. 8 shows Ramachandran plots for different temperatures. It is shown that the dihedral angles are mostly around the α-helix region. Ramachadran plots also suggest that dihedral angles corresponding to beta sheet conformation gradually appear as the temperature is increased, even though the absolute values for the fraction of beta contents from the DSSP analysis are less than 0.1%.

We have measured the extent of convergence of our simulation trajectory by calculating the visited area in PC space as a function of time. It is noted that the convergence is not completely reached and the last few ns trajectory seems to show partial convergence. The poor convergence may be due to the unstructured nature of the peptide in addition to the relatively short simulation time. In spite of relatively low convergence, consistent conformational characteristics can be obtained through the ensembles of various temperatures. The "Mean Structure Hypothesis" proposed by Zagrovic *et al*.[31] suggested that the representative structures, obtained from the unstructured conformational ensemble, may be related to the partially folded intermediate.

## Concluding Remarks

We have performed replica-exchange molecular dynamics

simulations on 41 residue peptide mainly composed of NAC (non Aβ component) sequence in α-synuclein. To investigate conformational characteristics of intrinsically unstructured peptides under different environments, we carried out structural analysis on the 'representative structures' for ensemble of structures occurring at different temperatures. Individual conformations obtained from the simulations of NAC peptide for various conditions show flexible structures close to random coil. Representative structures, by construction, contain collective information about ensemble of configurations obtained from the simulations. They can provide useful information about structural characteristics of intrinsically unstructured proteins. The secondary structure profile obtained from our simulations suggests that the NAC region of α-synuclein can be divided into roughly three helical-like segments. It can be argued that the monomeric state of the NAC peptide does not exhibit beta-like structures with random conformations of C-terminal region and potentially helical conformations of N-terminal region. Partial beta sheet conformation gradually appears as the temperature is increased. It is found that the overall helix-turn-helix like topology is relatively conserved even though the conformational fluctuations grow as the temperature increases. The coordinate-based and the distance-based representative structures exhibit noticeable differences at higher temperatures while they are similar at lower temperatures. It is found that structural variations for the coordinate-based representative structures are much larger, suggesting that distance-based representative structures provide more reliable information concerning characteristic features of intrinsically unstructured proteins. The present analysis also indicates that the conformational features of representative structures at high temperatures might be related to those in membrane or low pH environment.

**Acknowledgments.** This work was supported by grant R01-2006-000-10418-0 from the Basic Research Program of the Korea Science & Engineering Foundation. This work was also supported by the Korea Science & Engineering Foundation through the Center for Space-Time Molecular Dynamics (2008). KL wishes to acknowledge Stanford University for offering an opportunity to communicate with active researchers, especially Professor Wandless group. JP acknowledges the support by the Korea Research Foundation Grant (KRF-2003-070-C00026).

## References

1. Dobson, C. M. *Nature* **2003**, *426*, 884.
2. Ross, C. A.; Poirier, M. A. *Nat. Med.* **2004**, *10*, S10.
3. Skovronsky, D. M.; Lee, V. M.-Y.; Trojanowski, J. Q. *Annu. Rev. Pathol. Mech. Dis.* **2006**, *1*, 151.
4. Chiti, F.; Dobson, C. M. *Annu. Rev. Biochem.* **2006**, *75*, 333.
5. Fink, A. *Acc. Chem. Res.* **2006**, *39*, 628.
6. Uversky, V. N.; Oldfield, C. J.; Dunker, A. K. *Annu. Rev. Biophys.* **2008**, *37*, 215.
7. Dunker, A. K.; Lawson, J. D.; Brown, C. J.; Williams, R. M.; Romero, P.; Oh, J. S.; Oldfield, C. J.; Campen, A. M.; Ratliff, C. M.; Hipps, K. W.; Ausio, J.; Nissen, M. S.; Reeves, R.; Kang, C.; Kissinger, C. R.; Bailey, R. W.; Griswold, M. D.; Chiu, W.; Garner, E. C.; Obradovic, Z. *J. Mol. Graph. Modell.* **2001**, *19*, 26
8. Uversky, V. *Prot. Sci.* **2002**, *11*, 739.
9. Wright, P. E.; Dyson, H. J. *J. Mol. Biol.***1999**, *293*, 321.
10. Dyson, H. J.; Wright, P. E. *Curr. Opin. Struct. Biol.* **2002**, *12*, 54.
11. Ma, B.; Nussinov, R. *Curr. Opin. Chem. Biol.* **2006**, *10*, 445.
12. Teplow, D. B.; Lazo, N. D.; Bitan, G.; Bernstein, S.; Wyttenbach, T.; Bowers, M. T.; Baumketner, A.; Shea, J. E.; Urbanc, B.; Cruz, L.; Borreguero, J.; Stanley, H. E. *Acc. Chem. Res*. **2006**, *39*, 635.
13. Lücking, C. B.; Brice, A. *Cell. Mol. Life. Sci.* **2000**, *57*, 1894.
14. Spillantini, M. G.; Schmidt, M. L.; Lee, V. M.; Trojanowski, J. Q.; Jakes, R.; Goedert, M. *Nature* **2006**, *388*, 839.
15. Shults, C. W. *Proc. Natl. Acad. Sci. USA* **2006**, *103*, 1661.
16. Kim, S.; Seo, J.; Suh, Y. *Park. Rel. Dis.* **2004**, *10*, S9.
17. Eliezer, D.; Kutluay, E.; Bussell Jr., R.; Browne, G. *J. Mol. Biol.* **2001**, *307*, 1061.
18. Uversky, V. N.; Li, J.; Fink, A. L. *J. Biol. Chem.* **2001**, *276*, 10737.
19. Uversky, V. N. *J. Biomol. Struct. Dyn.* **2003**, *21*, 211.
20. Lee, I.-H.; Kim, H. J.; Lee, C.-H.; Paik, S. R. *Bull. Kor. Chem. Soc.* **2006**, *27*, 1001.
21. Ulmer, T. S.; Bax, A.; Cole, N. B.; Nussbaum, R. L. *J. Biol. Chem.* **2005**, *280*, 9595.
22. Iwai, A. I.; Yoshimoto, M.; Masliah, E.; Saitoh, T. *Biochemistry* **1995**, *34*, 10139.
23. Yoon, J.; Park, J.; Jang, S.; Lee, K.; Shin, S. *J. Biomol. Struct. Dyn.* **2008**, *25*, 505.
24. Cheatham III, T. E.; Cieplak, P.; Kollman, P. A. *J. Biomol. Struct. Dyn.* **1999**, *16*, 845.
25. Qiu, D.; Shenkin, P. S.; Hollinger, F. P.; Still, W. C. *J. Phys. Chem. A* **1997**, *101*, 3005.
26. Berendsen, H. J. C.; Postma, J. P. M.; van Gunsteren, W. F.; Di Nola, A.; Haak, J. R. *J. Chem. Phys.* **1984**, *81*, 3684.
27. Ponder, J. W. *TINKER: Software Tools for Molecular Design*, http://dasher.wustl.edu/tinker .
28. Kabsch, W.; Sander, C. S. *Biopolymers* **1983***, 22*, 2577.
29. McLachlan, A. D. *Acta Cryst A*. **1982**, *38*, 871.
30. Martin, A. C. R. *ProFit*, http://www.bioinf.org.uk/software/profit/.
31. Zagrovic, B.; Snow, C. D.; Khaliq, S.; Shirts, M. R.; Pande, V. S. *J. Mol. Biol.* **2002**, *323*, 153.
32. Lwin, T. Z.; Luo, R. *Protein Sci.* **2006**, *15*, 2462.
33. Feig, M.; MacKerell, Jr., A. D.; Brooks, III., C. L. *J. Phys. Chem. B* **2003**, *107*, 2831.
34. Freedberg, D. I.; Venable, R. M.; Rossi, A.; Bull, T. E.; Pastor, R. W. *J. Am. Chem. Soc.* **2004**, *126*, 10478.
35. Bisaglia, M.; Trolio, A.; Bellanda, M.; Bergantino, E.; Bubacco, L.; Mammi, S. *Protein Sci.* **2006**, *15*, 1408.
36. Yoon, S.; Welsh, W. J. *Protein Sci*. **2004**, *13*, 2149.
37. El-Agnaf, O.; Irvine, G. B. *J. Struct. Biol*. **2000**, *130*, 300.
38. Fink, A. L. In *Misbehaving Proteins: Protein (Mis)Folding, Aggregation, and Stability*; Murph, R. M.; Tsai, A. M., Eds.; Springer: 2006.
39. Uversky, V. N.; Li, J.; Fink, A. L. *J. Biol. Chem*. **2001**, *276*, 10737.
40. Giasson, B. I.; Murray, I. V. J.; Trojanowski, J. Q.; Lee, V. M.-Y. *J. Biol. Chem*. **2001**, *276*, 2380.
41. Lee, H. J.; Choi, C.; Lee, S. J. *J. Biol. Chem*. **2002**, *277*, 671.
42. Bisaglia, M.; Trolio, A.; Bellanda, M.; Bergantino, E.; Bubacco, L.; Mammi, S. *Protein Sci.* **2006**, *15*, 1408.